

# The Impact of Atmospheric Infrared Sounder (AIRS) Profiles on Short-term Weather Forecasts

Bradley T. Zavodsky<sup>\*a</sup>, Shih-Hung Chou<sup>b</sup>, Gary Jedlovec<sup>b</sup>, William Lapenta<sup>b</sup>

<sup>a</sup>University of Alabama in Huntsville, 320 Sparkman Drive, Huntsville, AL, 35805

<sup>b</sup>Marshall Space Flight Center, 320 Sparkman Drive, Huntsville, AL, 35805

## ABSTRACT

The Atmospheric Infrared Sounder (AIRS), together with the Advanced Microwave Sounding Unit (AMSU), represents one of the most advanced space-based atmospheric sounding systems. Aside from monitoring changes in Earth's climate, one of the objectives of AIRS is to provide sounding information with sufficient accuracy such that the assimilation of the new observations, especially in data sparse regions, will lead to an improvement in weather forecasts. The combined AIRS/AMSU system provides radiance measurements used as input to a sophisticated retrieval scheme which has been shown to produce temperature profiles with an accuracy of 1 K over 1 km layers and humidity profiles with accuracy of 10-15% in 2 km layers in both clear and partly cloudy conditions. The retrieval algorithm also provides estimates of the accuracy of the retrieved values at each pressure level, allowing the user to select profiles based on the required error tolerances of the application. The purpose of this paper is to describe a procedure to optimally assimilate high-resolution AIRS profile data in a regional analysis/forecast model. The paper focuses on a U.S. East-Coast cyclone from November 2005. Temperature and moisture profiles—containing information about the quality of each temperature layer—from the prototype version 5.0 Earth Observing System (EOS) science team retrieval algorithm are used in this study. The quality indicators are used to select the highest quality temperature and moisture data for each profile location and pressure level. AIRS data are assimilated into the Weather Research and Forecasting (WRF) numerical weather prediction model using the Advanced Regional Prediction System (ARPS) Data Analysis System (ADAS), to produce near-real-time regional weather forecasts over the continental U.S. The preliminary assessment of the impact of the AIRS profiles will focus on intelligent use of the quality indicators, analysis impact, and forecast verification against rawinsondes and precipitation data.

**Keywords:** SPoRT, AIRS, data assimilation, numerical weather prediction, quality control, forecast improvement, satellite-retrieved profiles, ADAS, WRF

## 1. INTRODUCTION

Significant weather events can often occur in regions downstream of sparse data (e.g. coastlines, deserts, large forests, etc.). Without adequate observations, meteorological analyses revert to the background (i.e. first guess) field, typically consisting of a previous gridded forecast. Observations from satellites are one valuable option to complement traditional atmospheric observations in these data sparse regions. Currently, the most state-of-the-art atmospheric profiler is the Atmospheric InfraRed Sounder (AIRS). AIRS radiances have been assimilated into global models yielding improvements in 5-day forecasts (e.g. Le Marshall et al. 2006, Garand et al. 2006, Jung et al. 2006). However, for centers focusing on regional forecasting problems—such as the SPoRT Center (Goodman et al. 2004)—impact of AIRS profiles on thermodynamic structures is a logical first step to using AIRS data. A methodology for assimilating AIRS profiles is presented herein.

Previously, Jedlovec et al. (2006) assimilated prototype version 5.0 AIRS thermodynamic profiles for a November 2005 U.S. East Coast cyclone case. Preliminary results from that case study showed that the AIRS data impacted the analysis and resulted in positive forecast impact on temperature and moisture when compared to a handful of East-Coast rawinsonde observations. This paper focuses on specific impacts of the AIRS data on the analyses and updated validation methodologies and forecast results from that same case study. Section 2 contains a description of the AIRS data used for this study. Section 3 contains a brief overview of the Advanced Regional Prediction System (ARPS; Xue et al., 2001) Data Assimilation System (ADAS; Brewster 1996) used to assimilate the AIRS profiles and the Weather

\*Brad.Zavodsky@nasa.gov; phone: 256 961-7914; fax: 256 961-7788; <http://weather.msfc.nasa.gov/sport/>

Research and Forecasting (WRF; Skamarock 2005) numerical model, which is used to produce the simulations. Section 4 describes the meteorological conditions of the case study and how the analysis and forecast model are coupled. Section 5 shows results of the impact of the AIRS profiles on the analyses. Section 6 shows the impact on temperature, moisture, and precipitation forecasts when the new model initial conditions containing added information from AIRS are used. Section 7 contains conclusions and future work.

## 2. AIRS DATA

### 2.1 AIRS Specifications

Aboard the EOS polar-orbiting Aqua satellite with an early afternoon equatorial crossing time, AIRS coupled with the Advanced Microwave Sounding Unit (AMSU) form an integrated temperature and humidity sounding system. AIRS is a cross-track scanning infrared spectrometer/radiometer with 2378 spectral channels between 3.7 and 15.4  $\mu\text{m}$  (650 and 2675  $\text{cm}^{-1}$ ). Due to its hyperspectral nature, AIRS can provide near-rawinsonde-quality atmospheric temperature profiles with the ability to resolve some small-scale vertical features. AIRS footprints coincide with AMSU footprints allowing AMSU data to be used in the retrieval process. This produces a uniform distribution of AIRS retrievals in both clear and partly cloudy scenes at a spatial resolution of approximately 50 km (Aumann et al. 2003). The superior vertical resolution and sounding accuracy make the instrument very appealing as a complement to rawinsonde measurements in data sparse regions.

For this study, a set of prototype version 5.0 soundings that contain improvements in the radiative transfer algorithm and quality control flags over the version 4.0 data currently available at the Goddard Distributed Active Archive Center (DAAC) are used. Each sounding contains approximately 54 vertical levels between 1013.25 and 100 hPa. Although these new version profiles have not yet been validated, it is expected that the relative validation errors will be similar to (or better than) those presented for the version 4.0 data (Susskind, personal communication). Globally, the AIRS version 4.0 retrieved profiles—compared to rawinsondes collocated in time and space—exhibit RMS errors of 1 K in 1-km layers for temperature and 10-15% RH in 2-km layers for moisture (Tobin et al. 2006, Divakarla et al. 2006). The lowest errors occur for clear-sky cases over water with degradation in profile accuracy in cloudy and/or over-land fields of view (FOVs).

### 2.2 Quality Indicators in Prototype Version 5.0 AIRS Data

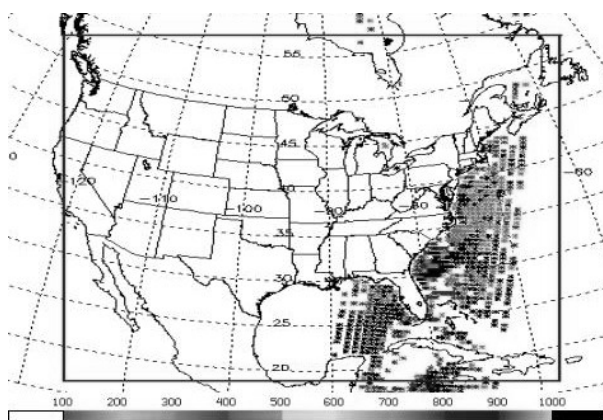


Fig. 1. Three-dimensional distribution of AIRS profile data assimilated at 0700 UTC 20 November 2005. Each point denotes the maximum pressure level corresponding to the level above which data is of good quality. The darkest black points represent the highest quality data. The rectangle denotes the bounds of the WRF/ADAS domain.

Each profile contains level-specific quality indicators allowing users to determine which parts of a profile are best for their applications. Because each retrieved profile is generated from the top of the atmosphere down, there is a specific level below which data is of questionable quality. This level is generally consistent with cloud tops and/or failures in cloud clearing but can also be attributed to faulty emissivity measurements over land. As an example, for low-level

clouds, the upper two-thirds of a profile may be valid; however, for thick convective clouds, an entire profile may be deemed questionable.

In this study, the quality indicators are used to select which levels of an AIRS sounding are to be assimilated into the analysis/forecast system. A plot of the three-dimensional distribution of AIRS profiles assimilated for this case study is shown in Figure 1. In the figure, temperature and moisture data above the indicated pressure level are used. The reader should refer to Susskind (2006) for a more detailed explanation of how the quality indicators are generated. Optimal use of these quality indicators will enable assimilation of only the highest quality data and is expected to yield improved forecasts in the 0- to 48-h time frame.

### **3. ANALYSIS AND FORECAST SCHEMES**

#### **3.1 ARPS Data Analysis System (ADAS)**

The ADAS provides a means to merge different sources of meteorological data into a coherent three-dimensional description of the atmosphere and has been configured to assimilate satellite profiles from AIRS. This particular analysis system was selected for its flexibility and ease of configuration for satellite-derived atmospheric profiles. In this study, only AIRS data are used to produce the analyses. No other data sets (e.g. rawinsondes, surface observations, aircraft observations, etc.) are assimilated.

The ADAS uses a Bratseth (1986) successive correction methodology that employs a ratio of the background and observation error covariances to calculate each analyzed field. These covariances are a combination of instrument/model error and representativeness error (i.e. error attributed to inaccuracies introduced due to differences between the resolution of the observations and the grid resolution). The error covariances used for the background are standard short-term forecast errors cited in the ADAS documentation, and the error tables used for the AIRS profiles are based on estimates cited by Tobin et al. (2006) for a Tropical Western Pacific (TWP) validation experiment of version 4.0 profiles. For reference, the observations covariance values for AIRS temperature are half that of those typically assigned to rawinsondes, and the observation covariance values for AIRS moisture are approximately one and a half times greater than those typically assigned to rawinsondes.

Horizontal and vertical scaling factors, which determine the amount of smoothing for each observation in the analysis, were also configured. Scaling factors should be selected such that information from enough observations can be combined without the data becoming decorrelated over large scaling distances. The horizontal scaling factors are reduced in subsequent iterations to ensure convergence (Lazarus et al. 2002). Three iterations of the Bratseth scheme are performed with horizontal scaling factors of 150, 120, and 100 km, respectively. The vertical scaling factors smooth data between pressure levels. Based on the vertical resolution of the data and the layer-averages that each AIRS level represents, this value is fixed at 750 m for the first two iterations and reduced to 400 m for the final iteration. The largeness of the vertical scaling factor mitigates some of the impact of using layer-averaged data in a fashion similar to point data. Again, for reference, rawinsondes typically are scaled at 300 km and 120 km in the horizontal and 500 m and 300 m in the vertical, further illustrating the finer horizontal resolution and layer nature of the AIRS profiles. For a more detailed discussion of how the analysis scheme is configured refer to Jedlovec et al. 2006.

#### **3.2 Weather Research and Forecasting (WRF) Model**

The forecast model used herein is the WRF (Skamarock 2005) model, a next-generation mesoscale numerical weather prediction system designed to serve both operational forecasting and atmospheric research needs. It is a limited-area, non-hydrostatic primitive equation model with multiple physical parameterization options. The model domain consists of a 150 x 120 grid with 36-km spacing and covers the contiguous United States, Western Atlantic Ocean, and Gulf of Mexico (see Fig. 1). It has 37 staggered terrain-following vertical levels with the top-level pressure at 100 hPa and finest resolution near the boundary layer.

The WRF physical options used in this study consist of the Ferrier (new Eta) microphysics, the Kain-Fritsch cumulus convection scheme (Kain and Fritsch 1990), and the Yonsei University (YSU) planetary boundary layer scheme (Hong et al. 2006). The rapid radiative transfer model (RRTM, Mlawer et al. 1997) and Dudhia scheme (Dudhia 1989) are

used for longwave and shortwave radiation, respectively, while the four-layer Noah land surface model (Chen and Dudhia 2001) provides the land surface physics.

## 4. EXPERIMENTAL DESIGN

### 4.1 Case Study: 20-22 November 2005

A disturbance over the Northern Gulf of Mexico at 1200 UTC 20 November 2005 played a significant role in the weather along the East Coast of the United States over the following two days. The storm system produced 6-h precipitation totals upwards of 65 mm ( $\approx 2.5$  in.) along its track over the coastal Atlantic states.

The synoptic maps in Figure 2 show 24-h snapshots—generated by the National Centers for Environmental Prediction (NCEP) and the National Weather Service—of the storm development from 1200 UTC 20 November 2005 to 1200 UTC 22 November 2005. At 1200 UTC 20 November 2005, a ridge of high pressure blanketed most of the Eastern seaboard, and a deep upper-level trough was propagating across the middle of the continent with the aforementioned shortwave over the central Gulf of Mexico. Twenty-four hours later, as the upper-level trough entered the Eastern states, the surface low began to deepen over Florida and Georgia. The storm moved quickly up the coast and deepened to 980 hPa by 1200 UTC 22 November off the coast of Delaware and New Jersey.

This particular storm system is of interest because of its proximity to the Southeastern United States and its genesis in a relatively data void region (over the Gulf of Mexico and Western Atlantic Ocean). It is anticipated that in this situation, the AIRS profiles should have their most significant impact on the ADAS analyses used to initialize the WRF. Another positive feature of this case study is that there is an Aqua overpass at a time prior to storm development and in the location of the storm path (i.e. there are plenty of clear and partly cloudy skies in the Gulf and western Atlantic providing good coverage of high-quality AIRS data).

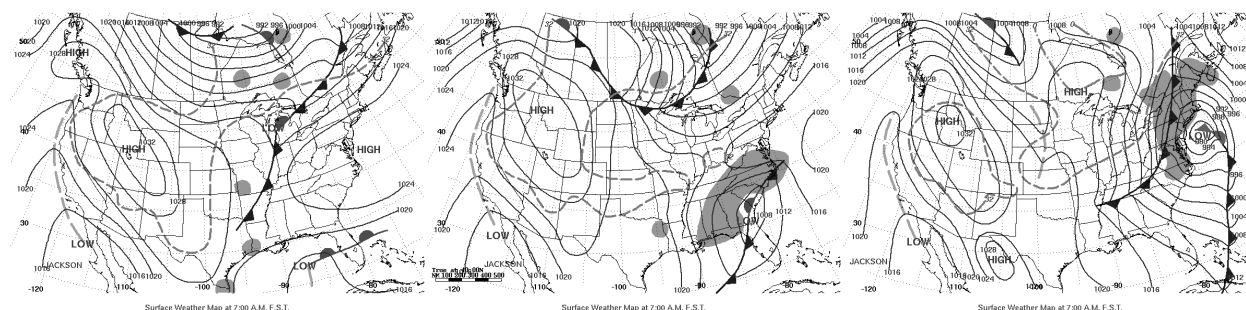


Fig. 2. Surface weather maps showing the development/track of a low-pressure system from the Gulf of Mexico across northern Florida and southern Georgia and into the Atlantic Ocean south of Long Island after 48 hours. The left-most panel shows conditions at 1200 UTC 20 November 2005, the center panel shows conditions at 1200 UTC 21 November 2005, and the right-most panel shows conditions at 1200 UTC 22 November 2005.

### 4.2 ADAS/WRF Coupling

The forecast/analysis cycle for the AIRS-assimilated runs is shown in Figure 3. The WRF is initialized with the North American Mesoscale (NAM) model analysis, which is available every 6 hours. The boundary conditions are updated every 3 hours using the NAM forecasts. The WRF/ADAS assimilation cycle begins at 0000 UTC 20 November 2005 with a 7-h forecast. Although there is a NAM analysis available at 0600 UTC, the earlier initialization time is selected because tests have shown that the 0000 UTC forecast produces a more reliable background field. In addition, using an earlier initialization allows the model to more properly adjust dynamically prior to data assimilation. This 7-h forecast is then used as the first guess field for the ADAS analysis at 0700 UTC when the AIRS profiles in the forecast domain are valid. The ADAS analysis initializes the WRF for the AIRS-assimilated runs and produces a total forecast of 48 hours. The control run is performed in the same manner except no data are assimilated within the ADAS. With the 48-h forecast, 3 sets of verification statistics are performed using East Coast rawinsonde observations at 12-h intervals.

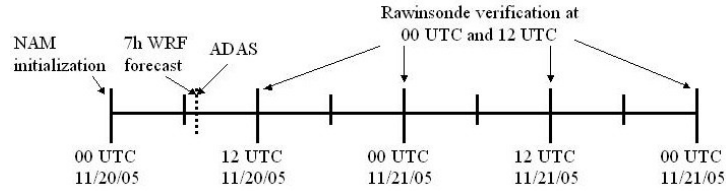


Fig. 3. ADAS/WRF forecast cycle schematic.

## 5. ANALYSIS IMPACT

The first step in investigating the impact of a new data set on an analysis is by examining the magnitude of the differences at various levels. For a new data set to have the potential to improve numerical forecasts, the observations must differ from the background field. If the observations are similar to the background field, then there are negligible changes to the initial model fields resulting in little or no impact to the resultant forecast. Figure 4 shows the impact of the AIRS data on the background field for 700 hPa temperature and dew point temperature.

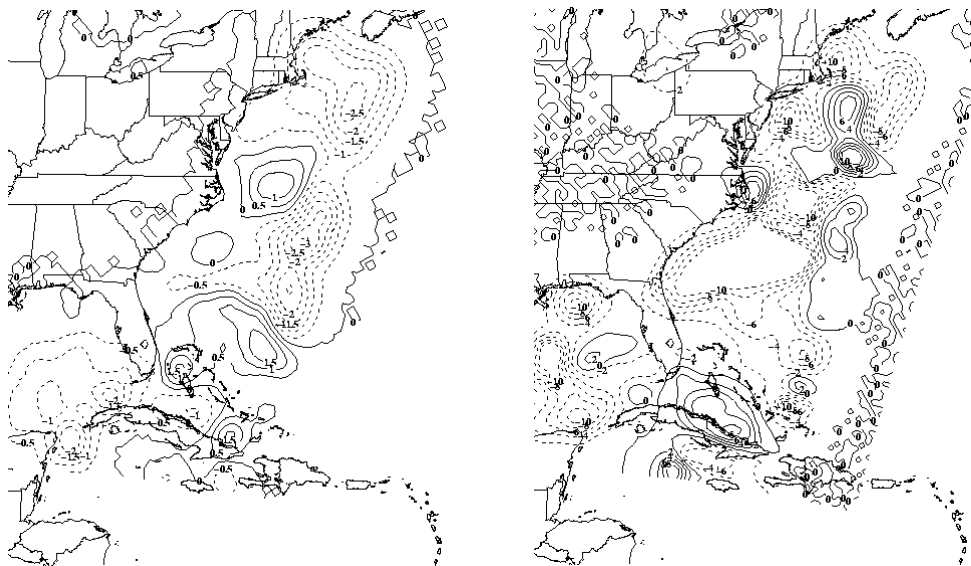


Fig. 4. 700 hPa ADAS analysis differences (AIRS-background) of temperature ( $^{\circ}\text{C}$ ; left) and dew point temperature ( $^{\circ}\text{C}$ ; right) showing the large scale cooling and drying effect of AIRS profiles on the analysis. In the figures, negative values (represented by dashed contours) represent cooling and drying. Analyses are valid at 0700 UTC 20 November 2005.

The spatial distribution and absolute magnitude of the changes at 700 hPa are representative of these differences at other vertical levels (not shown). AIRS profiles at 700 hPa have an overall cooling and drying impact over most of the region of assimilated data. Also, note that any changes over land are very small indicating that the analysis is changing only in the region where there is data, which adds confidence that the analysis scheme is performing as expected. The absolute magnitude of these changes reaches as high as  $\pm 3^{\circ}\text{C}$  for temperature and  $\pm 10^{\circ}\text{C}$  for dew point temperature. The impact of the AIRS data is relatively large, but it is necessary to test if the AIRS profiles are having a positive or negative impact on the model initial conditions. One way to test this is to compare to spatially collocated rawinsondes.

Because the AIRS data are valid at 0700 UTC, and there are no rawinsonde observations at this time, a qualitative assessment must be made of how well the AIRS data captures the change in atmospheric conditions at the sounding location between 0000 UTC and 1200 UTC. With the storm system approaching, one would expect a rapidly changing environment, and if the AIRS profiles are to add benefit to the initial model conditions they should represent this changing environment between the 0000 UTC and 1200 UTC rawinsonde observations. Figures 5 and 6 show comparisons between the 0000 UTC and 1200 UTC rawinsonde observations and spatially collocated soundings of the background field, an AIRS profile, and the resultant analysis at two rawinsonde sites on the East Coast (Wallops Island, VA; WAL and Morehead City, NC; MHX). Based on the figures, AIRS data in each of these figures produces an

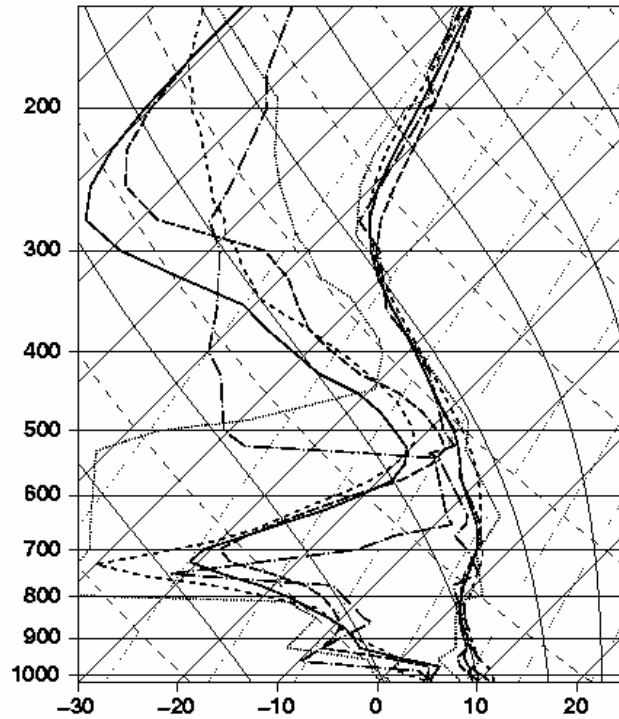


Fig. 5. Profiles of temperature (right group of lines) and dew point temperature (left group of lines) near Wallops Island, VA (WAL) rawinsonde location on 20 November 2005. The 0000 UTC rawinsonde is the dotted line, and the 1200 UTC rawinsonde is the dash/dot line. The background (long dash) and ADAS analysis (solid) profiles are for the nearest grid point to the rawinsonde location. The AIRS profile (short dash) is for the highest-quality retrieval closest to the grid point.

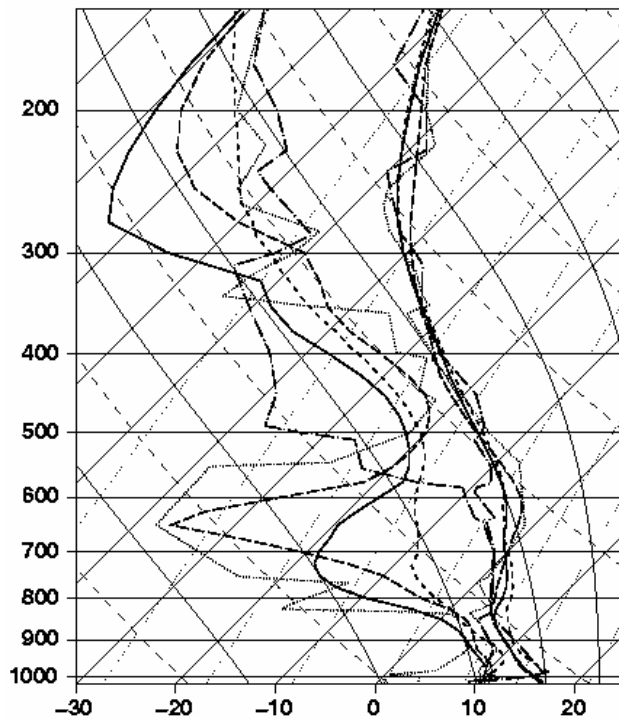


Fig. 6. Same as Fig. 5 but for Morehead City, NC (MHX) rawinsonde location.

analysis that more closely resembles the changing environment at 0700 UTC than the background for both temperature and moisture.

One surprising feature of the AIRS profiles is the detailed structure of both the temperature and moisture profiles. Specifically in Figure 5, it is apparent that AIRS correctly detects a relatively thin layer of very dry air between 850 and 700 hPa. This dry air is evident in the 0000 UTC rawinsonde and then to a lesser extent in the 1200 UTC rawinsonde. However, the moisture profile lies between the 0000 UTC and 1200 UTC rawinsonde values providing confidence as to the structure of the changing air mass at the AIRS observation time. The background field dew point temperature is too moist compared to the rawinsondes. The AIRS data do a good job of adjusting the analysis from the too-moist background field to a value that is more comparable to what would likely have been observed at 0700 UTC. These results are consistent with the drying at 700 hPa observed in Figure 4. Another feature seen in the moisture profiles in Figure 5 is the decrease in moisture between 300 and 500 hPa from the 0000 UTC and 1200 UTC rawinsondes. This moisture decrease is evident in both the AIRS data and subsequent ADAS analysis using the AIRS data; however, it is not well defined in the background field.

In advance of the storm system described in Section 4, there is a consistent cooling and moistening of the mid-troposphere between 700 and 500 hPa evident in the rawinsonde data in Figure 6. The background closely resembles the 0000 UTC rawinsonde observation, which is too warm and dry for the changing atmosphere at 0700 UTC. The AIRS profile data in this region successfully detects the cooling and moistening at these levels and adjusts the analysis towards cooler and moister conditions.

Because the AIRS profiles and resultant analyses are more representative of the changing environment between 0000 UTC and 1200 UTC, it appears that the AIRS profiles are improving the initial conditions used by WRF.

## 6. FORECAST IMPACT

Forecast impact for this case study are evaluated in two ways: 1) statistics between model output and East-Coast rawinsondes for temperature and dew point temperature verification and 2) threat scores between model output and NCEP Stage IV precipitation data—which are an analysis of radar and rain gauge data—for 6-h cumulative precipitation verification. Both sets of verifications occur on the East Coast since this is where the weather of interest occurred.

### 6.1 Temperature and Moisture Forecast Verification

The upper-air verification statistics for the 48-h forecast (at 12 hour intervals coincident with rawinsonde launches) are computed by comparing the rawinsonde value to the model forecast values interpolated to the location of that specific observation. In this study, verifications are based on 17 rawinsonde stations on the East Coast of the United States (see Fig. 7), which is where the storm system in the case study is impacting and where AIRS data will have the largest impact on the 0- to 48-h forecast.

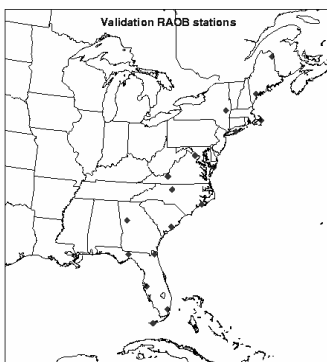


Fig. 7. Rawinsonde locations for verification study.

Results for the 48-h forecast are presented in Figure 8. Temperature is shown in standard bias (forecast minus rawinsonde) and root mean square error (RMSE), while moisture is shown in relative values, which are the standard value normalized by the average observation value. This is done to compensate for low moisture content in the upper levels. The relative bias (forecast minus rawinsonde) and RMSE for mixing ratio are defined as

$$rel\_bias = \left[ \frac{1}{N} \sum (fcst - obs) \right] / \left[ \frac{1}{N} \sum obs \right], \quad (1)$$

$$rel\_RMSE = \left[ \frac{1}{N} \sum (fcst - obs)^2 \right]^{1/2} / \left[ \frac{1}{N} \sum obs^2 \right]^{1/2}, \quad (2)$$

where N is the total number of observations at a given pressure level.

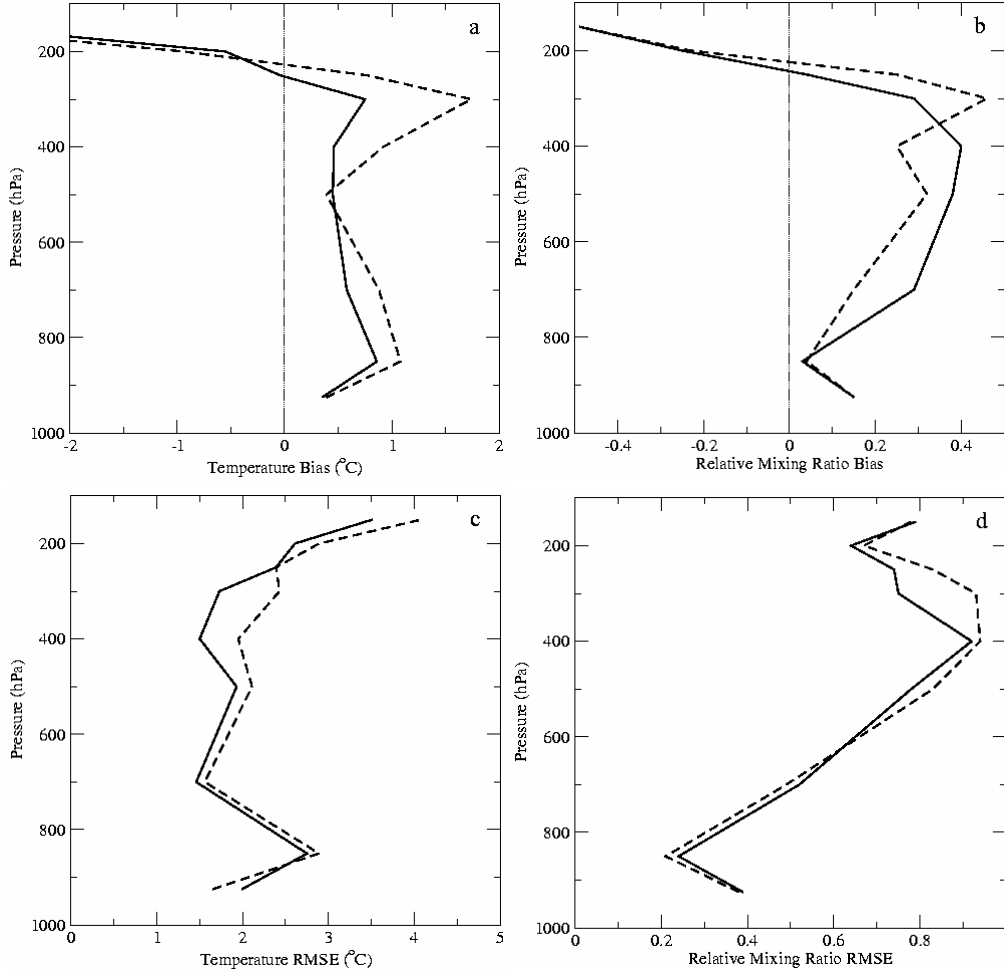


Fig. 8. 48-h forecast temperature a) bias (forecast – rawinsonde) and c) RMSE and mixing ratio b) bias (forecast – rawinsonde) and d) RMSE valid at 0000 UTC 22 November 2005. The dashed line represents the CNTL case; the solid line represents the AIRS case.

Overall, the 48-h forecast for the control is too warm and moist. For every level except the upper level, the addition of AIRS data (dashed line) cools the temperature throughout the troposphere by as much as 0.5°C for the 48-h forecast (Fig. 8a). This is consistent with the alterations to the initial conditions caused by assimilating the AIRS profiles (see Fig. 4). For the mixing ratio, biases are unchanged in the lowest layers but increased in the middle levels. Some decrease in bias is seen in the upper levels (Fig. 8b). Temperature RMS error is reduced by 0.2–0.5°C above 700 hPa; however, below 700 hPa there appears to be little change (Fig. 8c). Similarly, mixing ratio RMS error is reduced above 600 hPa with little change below that level (Fig. 8d). Part of the slight decrease in mixing ratio RMS error below 600 hPa may be the



result of moisture observations with larger errors that may have not been removed in the quality control process because only temperature error is considered for removal of data (Susskind, personal communication).

### 6.2 Precipitation Forecast Verification

Verification of precipitation forecasts are made by comparing the model output precipitation fields with 4-km NCEP Stage IV radar 6-h composite data mapped to the WRF model domain for direct comparison using grid points that lie to the east of 90°W longitude. While this provides ample verification data, there are some limitations to using Stage IV data. Foremost, much of the verification data is constrained to over-land regions because of radar and rain gauge locations, while much of the anticipated impact on the forecasts is expected over water. Precipitation is verified using bias scores and equitable threat scores (ETS) (Gandin and Murphy 1992) based on the amount of precipitation larger than various numerical thresholds. The bias score is a ratio of the number of observed points to the number of forecasted points that exceed the threshold value and is a measure of how accurate the forecast predicts the precipitation coverage. A bias score of 1 indicates perfect precipitation coverage while a value less (more) than 1 indicates under (over) forecasting of precipitation over the grid. The ETS indicates how well the forecasted rainfall region matches the observed rainfall region that exceeds a given threshold. Higher ETS indicates more accurate forecasts of precipitation location and intensity. An ETS of 1 indicates that the precipitation fields are perfectly aligned, and an ETS of 0 means that there are no matches at all. Near-zero ETS scores may also be indicative of very few observed and forecasted points.

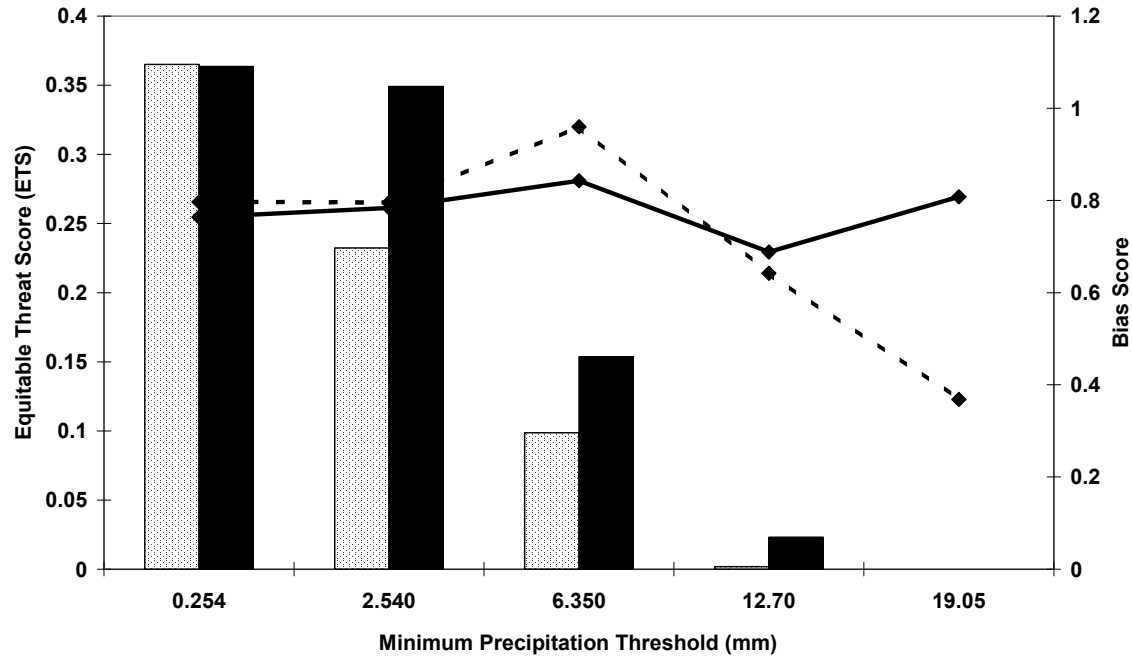


Fig. 9. Equitable Threat Score (ETS; bars) and Bias Scores (lines) for 6-h cumulative precipitation ending at 0000 UTC 22 November 2005 (48-h forecast). The dotted black bars and dashed black line represent the CNTL run, and the solid bars and solid line represent the AIRS run.

Figure 9 shows the bias score and ETS for 6-h cumulative precipitation totals ending at the 48-h forecast (valid at 0000 UTC 22 November 2005). The 48-h forecast is representative of the overall trends in the precipitation forecast for this case study. The bias scores indicate that the forecasts for both the CNTL and AIRS case slightly underestimate precipitation coverage for light to moderate thresholds. The AIRS case has slightly worse bias at lower precipitation thresholds, but outperforms the control for the moderate precipitation thresholds. For ETS, the AIRS case outperforms the CNTL case at every threshold except for the smallest (i.e. trace) where the two cases are approximately equal. Overall, the combination of the ETS and bias scores indicates that addition of AIRS profiles results in positive impact on the precipitation forecast for this case.

## 7. CONCLUSIONS/FUTURE WORK

This paper has presented a methodology for assimilating prototype version 5.0 AIRS thermodynamic profiles into a regional model. Quality indicators were used to select the highest-quality AIRS profile data in both clear and partly cloudy conditions. The ADAS was used to assimilate the AIRS data using a 7-h WRF forecast initialized with the NAM as a background. The resultant analysis was then used to initialize a 48-h model run. Results indicate that temperature and moisture forecasts are improved with the use of AIRS data when compared to collocated East-Coast rawinsondes. Similarly, accuracy of precipitation forecasts was shown to improve with the use of the highest quality AIRS data.

Future work will involve a near-real-time assimilation of AIRS data in a methodology similar to the one described herein. These assimilation projects will use thermodynamic profiles from version 5.0 of the EOS algorithm, which will be available in near real time in spring of 2007. These near-real-time forecasts will be run for a month or more to generate long-term statistics of temperature, moisture, and precipitation impact that will be more conclusive than the results from a single case. Along with the verification procedure outlined in this document, a more large-scale verification of temperature, moisture, height, and winds using grid point to grid point comparisons between our WRF forecasts and NAM analyses collocated in time. These comparisons provide a methodology for verifying model impact over water where upper air observations are not readily available.

## ACKNOWLEDGMENTS

This work is supported by Dr. Tsengdar Lee of NASA Headquarters. The authors would like to thank Kate LaCasse, Jonathan Case, Tim Miller, and Will McCarty for their assistance and input on this project.

## REFERENCES

1. J. Le Marshall, J. Jung, J. Derber, R. Treadon, M. Goldberg, W. Wolf, and T. Zapotocny, "Assimilation of Advanced InfraRed Sounder (AIRS) observations at the JCSDA". *Preprints, 14th Conference on Satellite Meteorology and Oceanography*, Atlanta, GA, Amer. Meteor. Soc., CD-ROM, 9.2 (2006).
2. L. Garand, A. Beaulne, and N. Wagner, "Assimilation of AIRS hyperspectral radiances at MSC". *Preprints, 14th Conference on Satellite Meteorology and Oceanography*. Atlanta, GA, Amer. Meteor. Soc., CD-ROM, P5.13 (2006).
3. J. A. Jung, T. H. Zapotocny, R. E. Treadon, and J. F. Le Marshall, "Atmospheric Infrared Sounder Assimilation Experiments Using NCEP's GFS". *Preprints, 14th Conference on Satellite Meteorology and Oceanography*. Atlanta, GA, Amer. Meteor. Soc., CD-ROM, P5.11 (2006).
4. S. J. Goodman, W. M. Lapenta, G. J. Jedlovec, J. C. Dodge, and T. Bradshaw, "The NASA Short-term Prediction Research and Transition (SPoRT) Center: A collaborative model for accelerating research into operations". *Preprints, 20th Conference on Interactive Information Processing Systems (IIPS)*, Seattle, WA, Amer. Meteor. Soc., CD-ROM, P1.34 (2004).
5. G. Jedlovec, S. H. Chou, B. T. Zavodsky, and W. Lapenta, "The use of error estimates with AIRS profiles to improve short-term weather forecasts". *SPIE Conference Proceedings 62331B* (2006).
6. M. Xue, K. K. Droegemeier, and V. Wong, "The Advanced Regional Prediction System (ARPS) - a multiscale nonhydrostatic atmospheric simulation and prediction tool. Part I: Model dynamics and verification". *Meteor. Atmos. Phys.*, 75, 161-193 (2001).
7. K. Brewster, K., "Implementation of a Bratseth analysis scheme including Doppler radar". *Preprints, 15th Conf. on Weather Analysis and Forecasting*. Amer. Meteor. Soc., Boston, MA, 596-598 (1996).
8. W. C. Skamarock, J. B. Klemp, J. Dudhia, D. O. Gill, D. M. Barker, W. Wang and J. G. Powers, "A Description of the Advanced Research WRF Version 2", NCAR Tech Note, NCAR/TN-468+STR, 88 pp.

[Available from UCAR Communications, P.O. Box 3000, Boulder, CO, 80307; on-line at: [http://box.mmm.ucar.edu/wrf/users/docs/arw\\_v2.pdf](http://box.mmm.ucar.edu/wrf/users/docs/arw_v2.pdf)] (2005).

9. H. H. Aumann, M. T. Chahine, C. Gautier, M. D. Goldberg, E. Kalnay, L. M. McMillin, H. Revercomb, P. W. Rosenkranz, W. L. Smith, D. H. Staelin, L. L. Strow, and J. Susskind, "AIRS/AMSU/HSB on the Aqua Mission: Design, Science Objectives, Data Products, and Processing Systems". *IEEE Transactions on Geoscience and Remote Sensing*, 41, 253-264 (2003).
10. D. C. Tobin, H. E. Revercomb, R. O. Knuteson, B. M. Lesht, L. L. Strow, S. E. Hannon, W. F. Feltz, L. A. Moy, E. J. Fetzer, and T. S. Cress, "ARM site atmospheric state best estimates for AIRS temperature and water vapor retrieval validation". *J. Geophys. Res.*, 111, D09S14, 18 pp. (2006).
11. M. G. Divakarla, C. D. Barnet, M. D. Goldberg, L. M. McMillin, E. Maddy, W. Wolf, L. Zhou, and X. Liu, "Validation of Atmospheric Infrared Sounder temperature and water vapor retrievals with matched radiosonde measurements and forecasts". *J. Geophys. Res.*, 111, D09S15, 20 pp. (2006).
12. J. Susskind, "Improved soundings and error estimates using AIRS/AMSU data". SPIE Conference Proceedings 623319 (2006).
13. A. M. Bratseth, "Statistical interpolation by means of successive corrections". *Tellus*, 38A, 439-447 (1986).
14. S. M. Lazarus, C. M. Ciliberti, J. D. Horel, and K. A. Brewster, "Near-real-time applications of a mesoscale analysis system to complex terrain". *Wea. Forecasting*, 17, 971-1000 (2002).
15. J. S. Kain, and J. M. Fritsch, "A one-dimensional entraining/detraining plume model and its application in convective parameterization". *J. Atmos. Sci.*, 47, 2784-2802 (1990).
16. S-Y Hong, Y. Noh, and J. Dudhia, "A new vertical diffusion package with an explicit treatment of entrainment processes". *Mon. Wea. Rev.*, 134, 2318-2341 (2006).
17. E. J. Mlawer, S. J. Taubman, P. D. Brown, M. J. Iacono, and S. A. Clough, "Radiative transfer for inhomogeneous atmosphere: RRTM, a validated correlated-k model for the long-wave". *J. Geophys. Res.*, 102 (D14), 16663-16682 (1997).
18. J. Dudhia, "Numerical study of convection observed during the winter monsoon experiment using a mesoscale two-dimensional model". *J. Atmos. Sci.*, 46, 3077-3107 (1989).
19. F. Chen and J. Dudhia, "Coupling an advanced land-surface/hydrology model with the Penn State/NCAR MM5 modeling system. Part I: Model description and implementation". *Mon. Wea. Rev.*, 129, 569-585 (2001).
20. L.S. Gandin and A. H. Murphy, "Equitable skill scores for categorical forecasts". *Mon. Wea. Rev.*, 120, 361-370 (1992).